Published OnlineFirst July 24, 2015; DOI: 10.1158/1535-7163.MCT-15-0350

Small Molecule Therapeutics

Molecular Cancer Therapeutics

Antitumor Activity and Acquired Resistance Mechanism of Dovitinib (TKI258) in *RET*-Rearranged Lung Adenocarcinoma

Chan Woo Kang[1], Kang Won Jang[2], Jinyoung Sohn[2], Sung-Moo Kim[2], Kyoung-Ho Pyo[2], Hwan Kim[2], Mi Ran Yun[2], Han Na Kang[2], Hye Ryun Kim[3], Sun Min Lim[3], Yong Wha Moon[3], Soonmyung Paik[4,5], Dae Joon Kim[6], Joo Hang Kim[3,7], and Byoung Chul Cho[3,7]

Abstract

RET rearrangement is a newly identified oncogenic mutation in lung adenocarcinoma (LADC). Activity of dovitinib (TKI258), a potent inhibitor of FGFR, VEGFR, and PDGFR, in *RET*-rearranged LADC has not been reported. The aims of the study are to explore antitumor effects and mechanisms of acquired resistance of dovitinib in *RET*-rearranged LADC. Using structural modeling and *in vitro* analysis, we demonstrated that dovitinib induced cell-cycle arrest at G_0–G_1 phase and apoptosis by selective inhibition of RET kinase activity and ERK1/2 signaling in *RET*-rearranged LC-2/ad cells. Strong antitumor effect of dovitinib was observed in an LC-2/ad tumor xenograft model. To identify the acquired resistance mechanisms to dovitinib, LC-2/ad cells were exposed to increasing concentrations of dovitinib to generate LC-2/ad DR cells. Gene-set enrichment analysis of gene expression and phosphor-kinase revealed that Src, a central gene in focal adhesion, was activated in LC-2/ad DR cells. Saracatinib, an src kinase inhibitor, suppressed ERK1/2 phosphorylation and growth of LC-2/ad DR cells. Taken together, these findings suggest that dovitinib can be a potential therapeutic option for *RET*-rearranged LADC, in which acquired resistance to dovitinib can be overcome by targeting Src. *Mol Cancer Ther; 14(10); 2238–48. ©2015 AACR.*

Introduction

Lung cancer is the most common cause of cancer death worldwide (1). Although survival of lung cancer patients still remains poor, molecular targeted therapies, which block important oncogenic pathways, have made remarkable progress over the years, particularly in lung adenocarcinoma (LADC), which is the most common histologic subtype of lung cancer (2–4). Indeed, treatment with gefitinib or crizotinib in *EGFR* mutation–positive or *ALK*-rearranged advanced LADC, respectively, has led to unprecedented improvements in objective response rate and progression-free survival over cytotoxic chemotherapy (5). The prevailing concept of genomics-driven medicine based on remarkable efficacy of these targeted therapies and the expanding genomic landscape of LADC have led to a significant surge in the number of genotype-directed lung cancer trials in molecular subtypes defined by oncogenic driver mutations in *PIK3CA*, *HER2*, *BRAF*, and *ROS1* (1).

RET encodes the tyrosine kinase receptor of growth factors belonging to the glial-derived neurotrophic factor family. Recently, *RET* rearrangement, specifically fusion, has emerged as a new molecular subtype in LADC (6, 7). The prevalence of *RET* fusions has been estimated approximately 1.2% to 2.0% in LADC (6–11). Several *RET* fusions have been identified in LADC, including kinesin family member 5B (*KIF5B*)-*RET*, coiled-coil domain containing 6 (*CCDC6*)-*RET*, tripartite motif-containing 33 (*TRIM33*)-*RET*, and nuclear receptor coactivator 4 (*NCOA4*)-*RET*. Among all fusion variants, *KIF5B–RET* is the most common type of fusion involving *RET*, present in approximately 90% of cases reported to date (11). *RET* fusion was mutually exclusive with other oncogenic driver mutations, such as *EGFR*, *HER2*, *BRAF*, or *EML4–ALK* fusion (10–13). Furthermore, expression of exogenous KIF5B–RET induced morphologic transformation and anchorage-independent growth of NIH3T3 fibroblasts (7). These findings strongly suggest that targeted inhibition of *RET* oncogene might be a potential strategy in the treatment of *RET* fusion–positive LADC.

Small-molecule tyrosine kinase inhibitors (TKI), including vandetanib, sunitinib, and sorafenib, effectively inhibited *RET* fusion–positive LADC in preclinical models (7, 8, 10, 14, 15). Therefore, several clinical trials of RET inhibitors are ongoing in *RET* fusion–positive LADC. Recently, treatment of cabozantinib and vandetanib, which have RET inhibitory activity, resulted in

[1]Brain Korea 21 PLUS Project for Medical Science, Yonsei University College of Medicine, Seoul, Korea. [2]JE-UK Institute for Cancer Research, JEUK Co. Ltd., Gumi-City, Kyungbuk, Korea. [3]Division of Medical Oncology, Department of Internal Medicine, Yonsei University College of Medicine, Seoul, Korea. [4]Division of Pathology, University of Pittsburgh, Pittsburgh, Pennsylvania. [5]Severance Biomedical Science Institute, Yonsei University College of Medicine, Seoul, Korea. [6]Department of Thoracic and Cardiovascular Surgery, Yonsei University College of Medicine, Seoul, Korea. [7]Institute for Cancer Research, Yonsei Cancer Center, Yonsei University College of Medicine, Seoul, Korea.

Note: Supplementary data for this article are available at Molecular Cancer Therapeutics Online (http://mct.aacrjournals.org/).

C.W. Kang and K.W. Jang contributed equally to this article.

Corresponding Author: Byoung Chul Cho, Yonsei Cancer Center, Division of Medical Oncology, Yonsei University College of Medicine, 50 Yonsei-ro, Seodaemun-gu, Seoul 120-752, Korea. Phone: 822-2228-8126; Fax: 822-393-3562; E-mail: cbc1971@yuhs.ac

doi: 10.1158/1535-7163.MCT-15-0350

Published OnlineFirst July 24, 2015; DOI: 10.1158/1535-7163.MCT-15-0350

dramatic responses in patients with *RET* fusion–positive LADC (12, 16).

Dovitinib (TKI258) is a potent inhibitor of receptor tyrosine kinases, including fibroblast growth factor receptor (FGFR) 1–3, VEGFR 1–3, platelet-derived growth factor receptor (PDGFR)-β, which has shown antitumor and antiangiogenic effects in preclinical models of colon, breast, bladder, pancreatic, and renal cell cancers (17–19). However, antitumor activity of dovitinib in *RET*-rearranged LADC has not been reported, except for the fact that dovitinib inhibits the RET kinase at a range of 7 nmol/L in an *in vitro* kinase assay (ref: dovitinib investigator's brochure).

Herein, we show potent antitumor activity of dovitinib in preclinical models of *RET*-rearranged LADC. In addition, we report the mechanism of acquired resistance to dovitinib in *RET*-rearranged LADC.

Materials and Methods

Compounds, antibodies, and cell lines

Dovitinib was kindly provided by Novartis Institutes for Biomedical Research (Basel, Switzerland). Gefitinib, vandetanib, sorafenib, sunitinib, saracatinib, and PF-562,271 were purchased from Selleck Chemicals.

Antibodies against EGFR, p-EGFR, RET, p-RET (Y905), AKT, p-AKT (S473), ERK1/2, p-ERK1/2 (T202/Y204), Cyclin D1, p21, p27, FAK, p-FAK (Y397), Src, p-Src (Y416), PDGFRβ, c-KIT, FGFR3 and integrin β1, integrin β3, integrin β4, integrin β5, integrin α4, integrin α5 were purchased from Cell Signaling Technology. Rabbit polyclonal antibody to *RET* (p-Y1062; ab51103), p-FLT3 (Y589; ab171975) was purchased from Abcam. Anti-β-actin antibody was purchased from Sigma Aldrich.

LC-2/ad cells were obtained from RIKEN in September 2013, NCI-H1299 cells and HEK293 cells were obtained from ATCC in January 2013. Each cell line was cultured using the medium recommended by the suppliers and never cultured for more than 3 months. The cell lines have not been authenticated by the authors.

Plasmid constructs and transfection

The plasmids that express *KIF5B–RET*, *CCDC6–RET*, and *KRAS* G12V were purchased from Addgene. HEK293 cells were plated at a density of 0.5×10^5 per 60 mm dish 1 day before transfection. HEK293 cells were transfected with the appropriate expression plasmids using Polyjet transfection reagent (SignaGen), according to the manufacturer's instructions. Transfected HEK293 cells were cultured at 37°C for 24 hours and then treated with or without dovitinib for an additional 4 hours prior to lysis.

In silico modeling

The structure models of RET with dovitinib, sunitinib, and vandetanib were modeled by Glide version 5.8 (Schrödinger). All figures were drawn using PyMol software (Schrödinger).

Growth inhibition assay

For MTT assays, cultured cells were seeded into 96-well plates (3,000 cells per well). Twenty-four hours after seeding, serial dilutions of appropriate inhibitors were added to the culture. After 72 hours, 50 μL of MTT (5 mg/mL stock solution) was added and the plates were incubated for an additional 4 hours. The medium was discarded and the formazan blue, which was formed in the cells, was dissolved with 100 μL DMSO. The optical density was measured at 540 nm. Relative survival in the presence of drugs was normalized to DMSO control cells after background subtraction. For colony formation assays, cells were seeded into 6-well plates (2.5×10^4 cells per well) and treated with the agents indicated in RPMI1640 containing 10% FBS for 14 days. Compound treatments were replaced at least every 3 days during the assay. After 14 days, cells were fixed in 3% paraformaldehyde in PBS for 10 minutes at room temperature and stained with 0.5% crystal violet in 20% methanol for 20 minutes. Images were captured using flatbed scanner, and the cells were dissolved with 20% acetic acids in 20% methanol for 30 minutes. Assays were performed independently at least three times.

Apoptosis assay and cell-cycle assay

An apoptosis assay was performed using the Annexin V–FITC Detection Kit (BD Biosciences) according to the manufacturer's protocol. For the cell-cycle assay, 4.0×10^5 of LC-2/ad cells were fixed with cold-80% ethanol for 1 hour on ice. The cells were then centrifuged at 800 rpm for 5 minutes followed by resuspension in 1 mL of PI Master Mix containing 40 μL of propidium iodide (Life Technologies), 10 μL of RNase A (Sigma-Aldrich) and 950 μL of PBS. After incubation at 37°C for 30 minutes, DNA ploidy was analyzed by flow cytometry.

Immunoblotting

Preparation of whole-cell protein lysates and Western blot analysis were described previously. Briefly, cells were then chilled on ice, washed twice with ice-cold PBS, and lysed in a buffer (Cell Signaling Technology) containing 1 mmol/L phenylmethylsufonylfluoride and 1× protease inhibitors (Sigma Aldrich). Protein concentrations were determined using a Bradford Assay kit (Bio-Rad Laboratories). Equal amounts of protein in cell lysates were separated by SDS-PAGE, transferred to membranes, immunoblotted with specific primary and secondary antibodies, and the blot was detected by SuperSignal West Pico Chemiluminescent Substrate (Thermo Fisher Scientific), according to the manufacturer's instructions.

siRNA transfection

siRNA was synthesized by Invitrogen (The sequence of siRNA listed in Supplementary Table S2) and was transfected into the cells using Lipofectamine RANiMAX (Invitrogen) according to the manufacturer's instructions.

Human phospho-kinase array

The human phospho-kinase array kit (R&D Systems) was used to detect the activation of 49 different protein kinases mediating various aspects of cellular proliferation following the manufacturer's instructions. Briefly, LC-2/ad cells and LC-2/ad DR cells were plated in 10 cm dishes and cultured at 37°C for 28 hours. After cell lysis, 500 μg of lysate was applied to a membrane-anchored phosphor-kinase array and incubated at 4°C for 24 hours. Membranes were exposed to chemiluminescent reagents and detected by X-ray film (AGFA).

Establishment of dovitinib-resistant LC-2/ad cell line

LC-2/ad cells were cultured in increasing concentrations of dovitinib up to 5 μmol/L to generate polyclonal-resistant clones (LC-2/ad DR). After approximately 6 months, LC-2/ad DR cells with strong resistance to dovitinib (IC_{50} > 3 μmol/L) were established.

Published OnlineFirst July 24, 2015; DOI: 10.1158/1535-7163.MCT-15-0350

Xenograft studies

All animal experiments were carried out under an Institutional Animal Care and Use Committee–approved protocol and institutional guidelines for the proper and humane use of animals. Nude mice were injected subcutaneously with 5×10^6 LC-2/ad cells or LC-2/ad DR cells. Mice were randomized into groups of 7 animals and treated with either vehicle, vandetanib or dovitinib (oral, every day) for the indicated duration of treatment. The length, width, and depth of the tumor mass were measured every 2 days using calipers, and tumor volume was calculated as: tumor volume = 0.5236 × length × width × depth (mm^3). The rate of change in body weight (BW) was calculated using the following formula: $BW = W/W_0 \times 100$, where W and W_0 are the body weight on a specific experimental day and on the first day of treatment, respectively.

Microarray analysis and gene-set enrichment analysis

Total RNA was extracted using RNeasy columns (Qiagen) according to the manufacturer's protocol. Total RNA was amplified and purified using Target Amp-Nano Labeling Kit for Illumina Expression Bead Chip (EPICENTRE) to yield biotinylated cRNA according to the manufacturer's instructions. We used gene-set enrichment analysis (GSEA) to evaluate the genes comprising a specific gene signature are coordinately up- or down-regulated between LC-2/ad and LC-2/ad DR cells. Gene signatures queried included those deposited in C2 KEGG genesets collection in the Molecular Signatures Database (MSigDB; version 4.0; http://www.broadinstitute.org/gsea/msigdb/index.jsp). A gene set of Focal adhesion factors used in the analysis was constructed using 38 Focal adhesion core factors. The data discussed in this publication have been deposited in NCBI's Gene Expression Omnibus (20) and are accessible through GEO series accession number GSE69226 (http://www.ncbi.nlm.nih.gov/geo/query/acc.cgi?acc=GSE69226).

Statistical analysis

Quantitative results were analyzed by ANOVA or *t* test. Statistical significance was established for $P < 0.05$.

Results

Dovitinib inhibits RET kinase activity

Dovitinib, of which chemical structure was shown in Fig. 1A, targets type III, IV, and V RTKs, including PDGFRβ, CSF-1R, KIT, FLT3, VEGFR, TrkA, RET, and FGFRs. To explore *RET* fusion as an additional target indication of dovitinib, we first performed *in silico* modeling of *RET* with dovitinib and two other RET–TKIs, sunitinib and vandetanib (Fig. 1B). Docking score of *RET* kinase complex with dovitinib, sunitinib, and vandetanib were calculated using Glide (Supplementary Table S1 and Fig. 1B). Docking simulation showed almost identical docking structure for dovitinib and two other *RET*–TKIs. Dovitinib–RET complex exhibited high docking score (−9.16), which was comparable with those of sunitinib and vandetanib. The structure modeling suggested that dovitinib formed hydrogen bonds with A907 and Q905 sites, which are located within active site of the RET kinase. According to Novartis investigator's brochure, dovitinib inhibited RET in nanomolar range (7 nmol/L) an *in vitro* kinase assay. Together, these results strongly suggest that dovitinib has potential to inhibit RET kinase activity.

To determine whether dovitinib could inhibit kinase activity of the two most common type of fusions, *CCDC6–RET* and *KIF5B–RET*, we first transfected HEK293 cells with plasmids encoding each fusion variants. Cells were lysed after dovitinib treatment and exogenous expression of RET kinase tyrosine 905 (Y905) was determined by immunoblot analysis (Fig. 1C). Dovitinib suppressed the phosphorylation of Y905 in both CCDC6–RET and KIF5B–RET fusion kinases, resulting in significant reduction of ERK1/2 phosphorylation in CCDC6–RET or KIF5B–RET plasmid-transfected HEK293 cells. However, ERK1/2 phosphorylation was unaffected by dovitinib in HEK293 cells transfected with mutant $KRAS^{G12V}$ plasmids. Next, we examined whether dovitinib selectively inhibited RET activity, leading to decreased ERK1/2 phosphorylation, by transfecting either $KRAS^{G12V}$ or KIF5B–RET plasmids into HEK293 cells (Fig. 1D). The ERK1/2 phosphorylation induced by $KRAS^{G12V}$ transfection could not be suppressed by treatment with dovitinib, a RET–TKI (vandetanib) or a selective EGFR-TKI (gefitinib). On the other hand, dovitinib and vandetanib, but not gefitinib, potently inhibited phosphorylation of RET and ERK1/2 in KIF5B–RET transfected HEK293 cells. Taken together, these results indicate that dovitinib has ability to specifically inhibits RET kinase activity and ERK1/2 signaling mediated by RET.

Dovitinib induces cell-cycle arrest and apoptosis of *RET*-rearranged LADC via selective inhibition of *RET* kinase

LC-2/ad cells were recently reported to harbor the *CCDC6–RET* rearrangement. Silencing of RET expression by siRNA targeting RET significantly decreased phosphorylation of ERK1/2, a key molecule of RET downstream signaling, and cell viability in LC-2/ad cells (14, 15). These results indicate that CCDC6–RET plays an important role in the proliferation and survival of LC-2/ad cells.

Next, we evaluated the effect of dovitinib on the growth of the LC-2/ad cells. Compared with H1299 cells without *RET* rearrangement, dovitinib potently suppressed the growth of LC-2/ad (IC_{50} = 0.2 μmol/L), indicating selective antitumor effects of dovitinib against RET kinase activity (Fig. 2A). Consistent with the results of MTT assays, treatment of dovitinib suppressed the phosphorylation of RET and ERK1/2 in a dose-dependent manner (Fig. 2B). Moreover, dovitinib inhibited the expression of cyclin D1 and induced p21 (Fig. 2B), which was in parallel with the fact that dovitinib significantly induced cell-cycle arrest at G_0–G_1 phase (Fig. 2C). Furthermore, treatment of dovitinib significantly increased a subpopulation of the Annexin V–positive apoptotic cells (Fig. 2D).

As dovitinib is known to target multiple tyrosine kinases, the growth suppression effect of dovitinib in LC-2/ad may not be due to selective inhibition of RET kinase. To rule out this possibility, effects of dovitinib on other known targets were assessed in immunoblotting. As shown in Supplementary Fig. S1A, dovitinib inhibited RET phosphorylation at the dose of 0.01 μmol/L, whereas it did not affect FLT3 phosphorylation even at 1 μmol/L. The phosphorylation of FGFR and PDGFRβ were not detected in LC-2/ad. Consistent with the immunoblot analysis, the introduction of siRET in LC-2/ad significantly suppressed the proliferation, whereas siFGFR3, siPDGFRβ, siFLT3, and siKIT had no significant effect on cell viability (Fig. 2E and F).

Published OnlineFirst July 24, 2015; DOI: 10.1158/1535-7163.MCT-15-0350

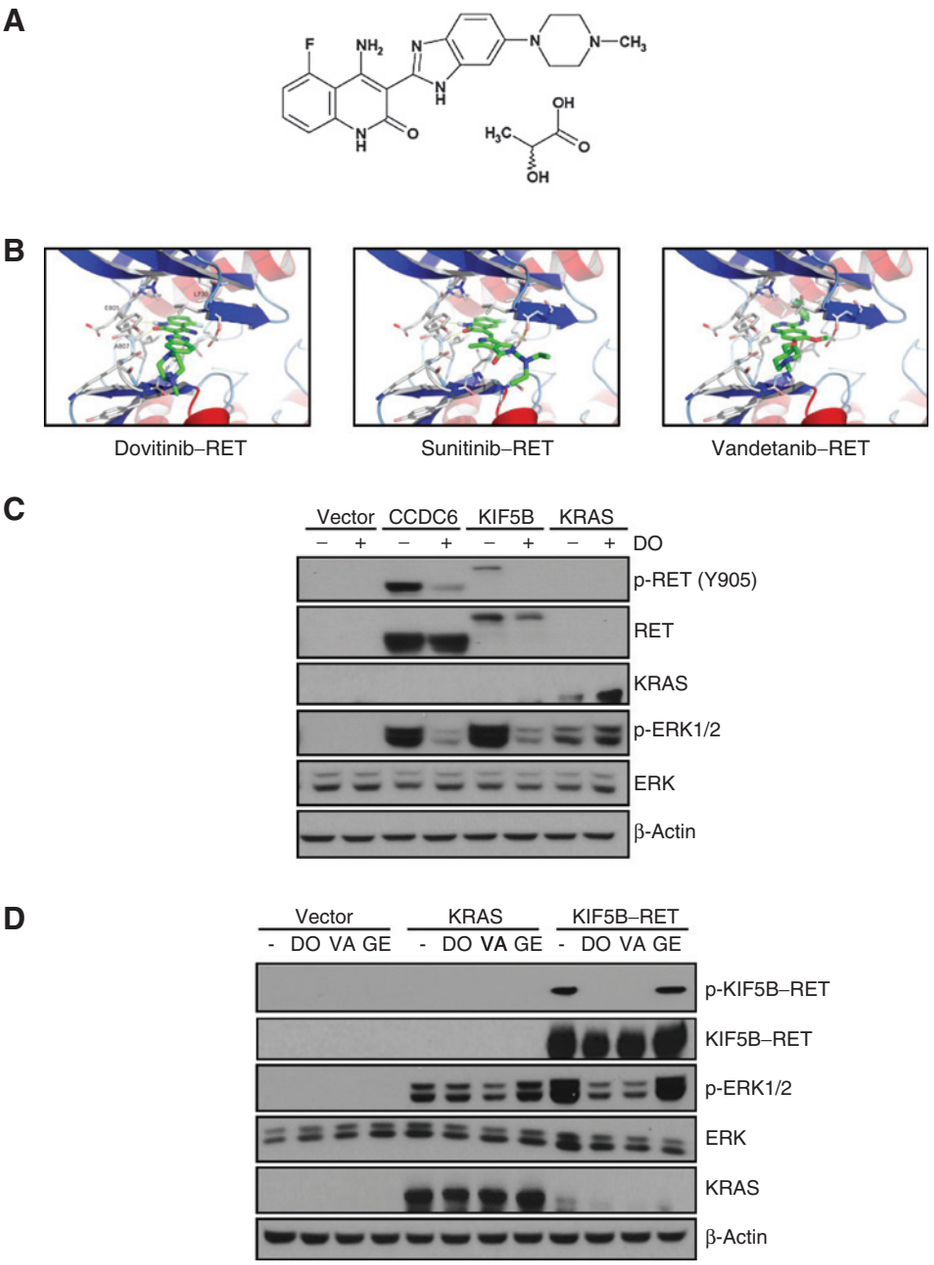

Figure 1.
Inhibition of RET-fusion kinase activity by dovitinib. A, chemical structure of dovitinib. B, X-ray structure of dovitinib with RET, sunitinib with RET, and vandetanib with RET. C, effects of dovitinib on the phosphorylation levels of RET in HEK293 cells expressing *CCDC6–RET*, *KIF5B–RET*, or KRAS. Each transfected HEK293 cell was treated with DMSO (−) or dovitinib 1 μmol/L (DO) for 4 hours. The expression levels of indicated protein levels were detected by Western blot analysis using the corresponding antibodies. D, Western blot analysis showing the effect of dovitinib (DO), vandetanib (VA), and gefitnib (GE) on expression of indicated proteins. Each transfected cell was treated with 1 μmol/L of indicated inhibitor for 4 hours.

Taken together, these results suggest that dovitinib induces cell-cycle arrest and cellular apoptosis via selective inhibition of RET kinase and its downstream signaling in lung cancer cells harboring *RET* rearrangement.

Dovitinib inhibits growth of *RET*-rearranged LADC more effectively than other RET–TKIs

We next compared antitumor effects of dovitinib with other known RET–TKIs, such as vandetanib, sunitinib, and sorafenib, using gefitinib, a selective EGFR–TKI, as a negative control. Contrary to gefitinib, dovitinib suppressed 100% inhibition of RET phosphorylation at the dose of 1 μmol/L. This was more evident in long-exposure blots (Fig. 3A). Moreover ERK1/2 and the expression of cyclin D1 inhibited by dovitinib, as potently as other known RET–TKIs (Fig. 3A). Notably, compared with other RET–TKIs, dovitinib exerted the most potent inhibitory effects on the proliferation of LC-2/ad cells in MTT assays (Fig. 3B). The superior antitumor activity of dovitinib to vandetanib, sunitinib and sorafenib in LC-2/ad cells became more evident through long-term (14 days) colony formation assays (Fig. 3C). Taken together, our data suggest that dovitinib inhibits growth of *RET*-rearranged LADC at least as effectively as other known RET–TKIs.

Antitumor activity of dovitinib in LC-2/ad xenograft models

To evaluate antitumor activity of dovitinib *in vivo*, we tested the effects of dovitinib and vandetanib on the growth

Published OnlineFirst July 24, 2015; DOI: 10.1158/1535-7163.MCT-15-0350

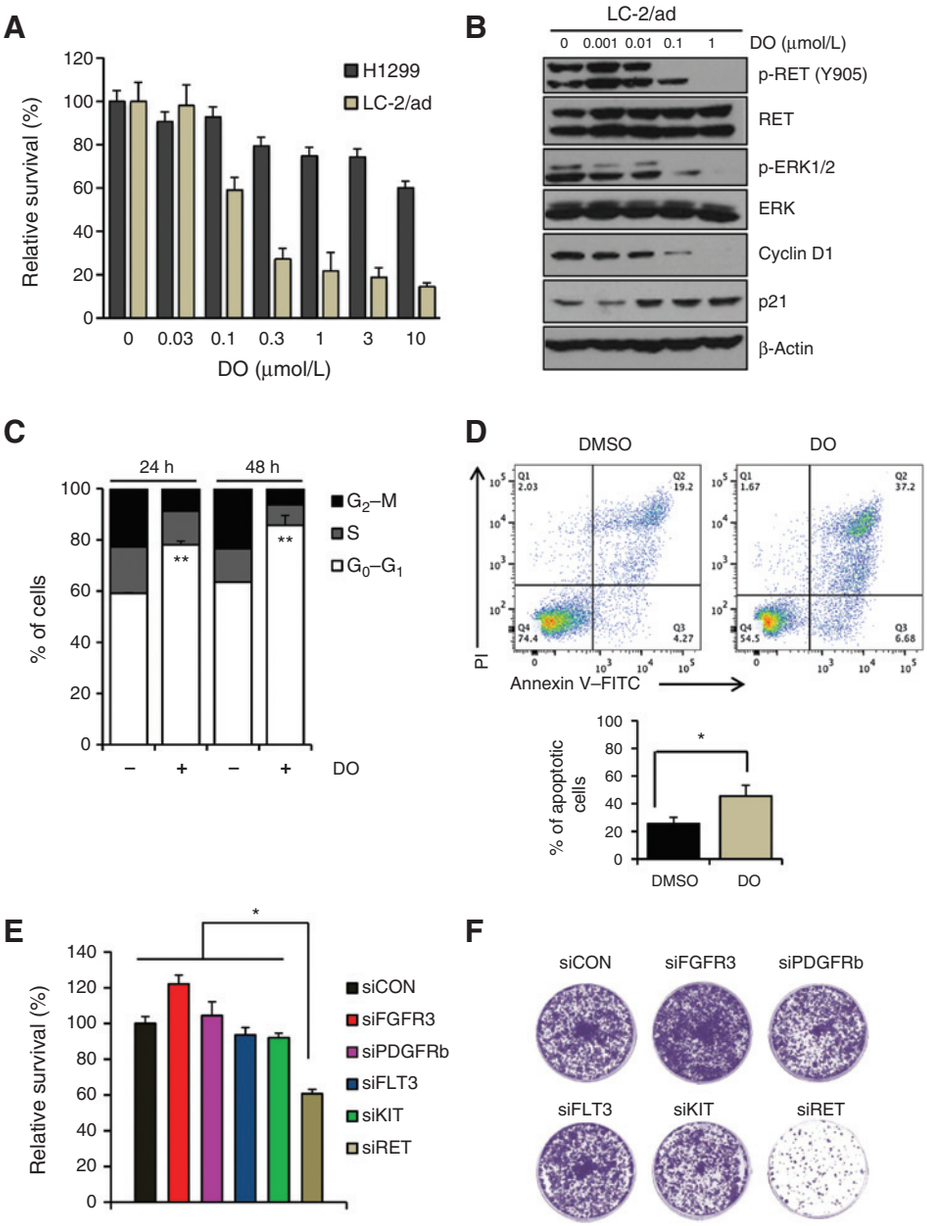

Figure 2.
Inhibition of *RET* fusion–driven tumors by dovitinib. A, relative survival of H1299 and LC-2/ad against dovitinib after 72 hours treated with dovitinib. B, Western blot analysis of *CCDC6–RET*, ERK1/2, and cyclin D1, p21, and β-actin in LC-2/ad cells after treated with dovitinib (DO) for 4 hours. C, LC-2/ad cells were treated with dovitinib 0.5 μmol/L (DO) for 24 or 48 hours. Cell-cycle distribution was measured by propidium iodide staining and subsequent FACS analysis. Error bars, mean ± SEM ($n = 3$). **, $P < 0.01$, vehicle (DMSO) versus DO (dovitinib) in both 24 and 48 hours. D, FACS analysis via the Annexin V/PI double-staining assay was used to observe the induction of apoptosis. After treating with DMSO or dovitinib 0.5 μmol/L (DO) for 72 hours, cells were stained with Annexin V-FITC/PI double staining. Error bars, mean ± SEM ($n = 3$). *, $P < 0.05$, DMSO versus dovitinib (DO). E, MTT assay of siCON, siFGFR3, siPDGFRb, siFLT3, siKIT, or siRET-transfected LC-2/ad cells. Indicated siRNA-transfected LC-2/ad cells were incubated for 72 hours before treating with MTT solution. F, colony formation assay of siCON, siFGFR3, siPDGFRb, siFLT3, siKIT, or siRET-transfected LC-2/ad cells. Indicated siRNA-transfected LC-2/ad cells were incubated for 14 days before staining with crystal violet.

of LC-2/ad xenograft tumors established in nude mice. Mice treated with dovitinib showed remarkable tumor regression at all doses without significant weight loss at 30 and 60 mg/kg doses of dovitinib (Fig. 4A and Supplementary Fig. S2A). Vandetanib at a dose of 50 mg/kg also produced similar efficacy, although mice were not tolerated well and experienced significant weight loss (Supplementary Fig. S2A). In waterfall plots, the percent volume changes of the individual tumors were greater in dovitinib treatment group compared with those in vandetanib group, showing complete tumor regression (−100%) in 3 of 7 mice treated with two different doses of dovitinib (Fig. 4B). Dovitinib suppressed phosphorylation of RET and ERK1/2 relative to vehicle treatment, as assessed by immunoblots and immunohistochemistry of tumor tissues from the xenograft (Fig. 4C and D). Taken together, our *in vitro* and *in vivo* findings confirm that dovitinib is effective against *RET* fusion–positive LADC.

Activation of Src mediates acquired resistance to dovitinib in LC-2/ad DR cells

In most targeted agents, acquired resistance eventually develops after an initial response (21). To identify potential mechanisms of acquired resistance to dovitinib, we established LC-2/ad DR cells with acquired resistance to dovitinib by exposing LC-2/ad cells to increasing doses of dovitinib. LC-2/ad DR cells showed strong resistance to dovitinib (IC_{50} > 3 μmol/L; Fig. 5A). Next, LC-2/ad and LC-2/ad DR cells were subjected to genome-wide gene expression profiling using

Published OnlineFirst July 24, 2015; DOI: 10.1158/1535-7163.MCT-15-0350

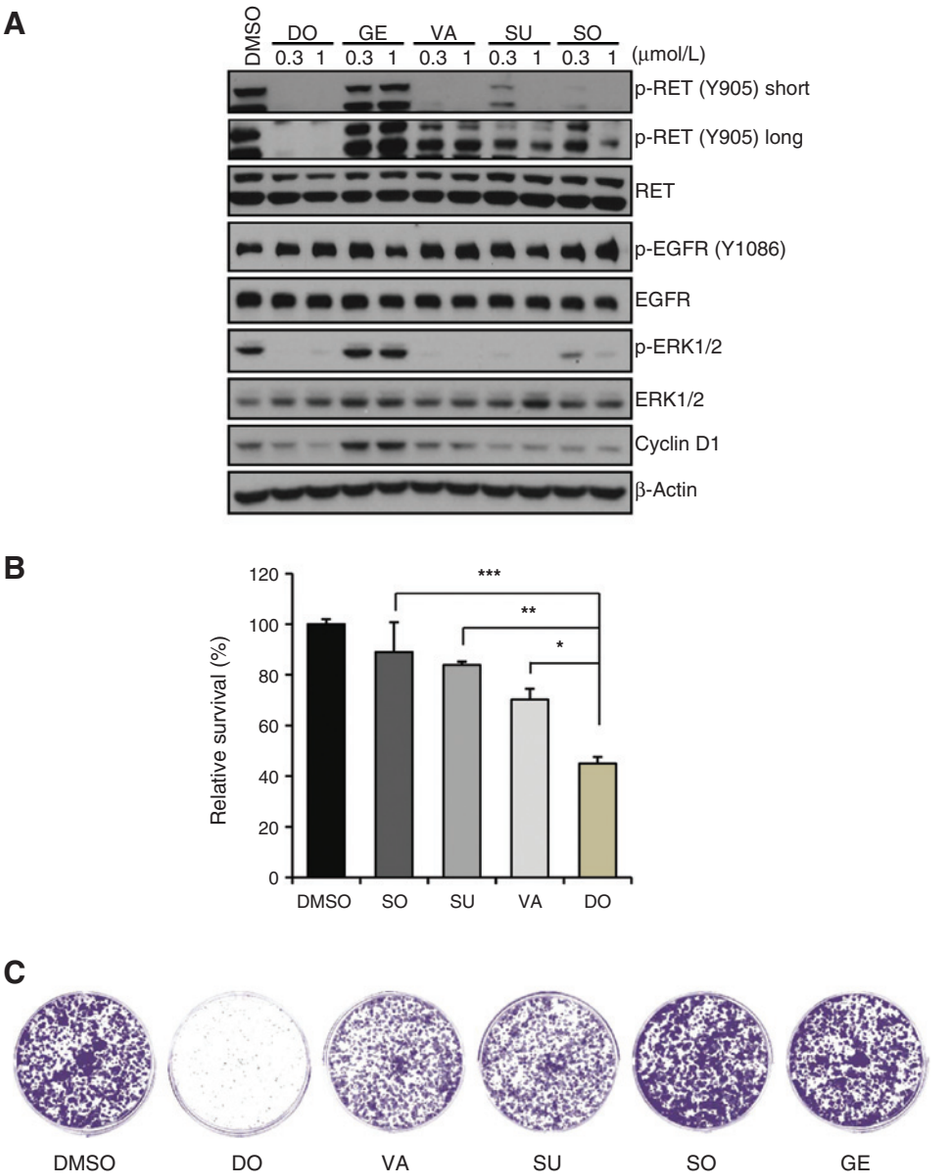

Figure 3.
Differences in the cell growth inhibition efficacy of *RET* fusion–driven NSCLC between dovitinib and other RET inhibitors. A, Western blot analysis of indicated markers in LC-2/ad cells after treated with dovitinib (DO), gefitinib (GE), vandetanib (VA), sunitinib (SU), or sorafenib (SO) for 4 hours. B, MTT assays of LC-2/ad. Cells were treated with 1 μmol/L sorafenib (SO), 1 μmol/L sunitinib (SU), 1 μmol/L vandetanib (VA), or 1 μmol/L dovitinib (DO) for 72 hours, and cell viability was determined using MTT (5 μg/mL) solution by measuring the absorbance at 540 nm in a microplate reader. Means are derived from five replicates ($n = 3$). Error bars, mean ± SE of three replicates. *, $P < 0.05$, vandetanib (VA) versus dovitinib (DO); **, $P < 0.01$; ***, $P < 0.001$, dovitinib (DO) versus sunitinib (SU) or sorafenib (SO) in LC-2/ad cells, respectively. C, colony formation assay of LC-2/ad cells. Cells were grown in the absence or presence of 0.5 μmol/L of indicated inhibitor for 14 days. All cells were fixed, stained with crystal violet (0.005%), and represent quantification.

cDNA microarray. GSEA against Kyoto Encyclopedia of Genes and Genomes (KEGG) database showed that focal adhesion pathway was significantly enriched, with Src contributing significantly to the core enrichment, in LC-2/ad DR cells, as compared with LC-2/ad cells (Fig. 5B). LC-2/ad DR cells displayed higher phosphorylation level of Src and focal adhesion kinase (FAK) in phospho-kinase array than LC-2/ad cells, which was confirmed by immunoblots (Fig. 5C and D). Increased Src activation in LC-2/ad DR cells led to constitutive ERK1/2 phosphorylation unresponsive to dovitinib treatment (Fig. 5D). Interestingly, contrary to LC-2/ad cells, LC-2/ad DR cells did not activate RET kinase any more, suggesting the loss of addiction to *RET* fusion in these cells (Fig. 5D).

Previous studies have demonstrated that Src sits on the signaling node mediating resistance to multiple anticancer agents (22). The increased activation of Src led us to hypothesize that Src activation directly mediated acquired resistance to dovitinib in LC-2/ad DR cells. To test this hypothesis, we inhibited Src activity using either saracatinib, a selective Src inhibitor, or siRNA targeting Src (siSrc) in LC-2/ad DR cells. Although dovitinib and other known RET–TKIs could not inhibit tumor growth in colony formation assays, saracatinib significantly exerted growth inhibitory effects on LC-2/ad DR cells (Fig. 6A). Furthermore, siSrc could efficiently inhibit tumor growth only in LC-2/ad DR cells (Fig. 6B). On the other hand, siRET could not inhibit tumor growth in LC-2/ad DR cells, suggesting the minimal role of RET signaling in survival of these cells (Fig. 6B). Consistent with cell viability data, inhibition of RET kinase by dovitinib or siRET abrogated ERK1/2 activity only in RET-dependent LC-2/ad cells, and inhibition of Src by saracatinib or siSrc abrogated ERK1/2 activity only in Src-dependent LC-2/ad DR cells (Fig. 6C and D).

Published OnlineFirst July 24, 2015; DOI: 10.1158/1535-7163.MCT-15-0350

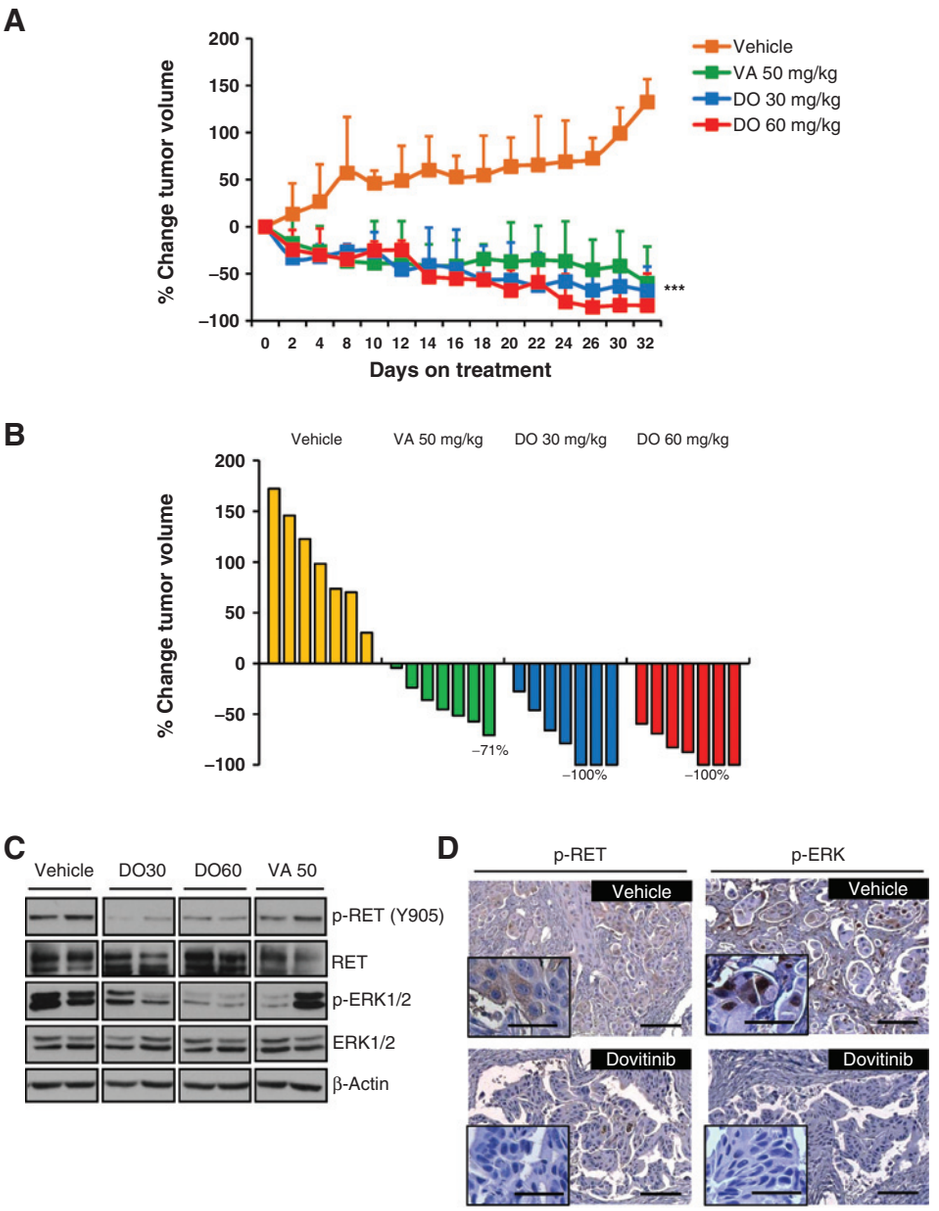

Figure 4.
Antitumor activity of dovitinib against *RET* fusion–driven tumors. A, mice bearing LC-2/ad cells were treated with vehicle only (Vehicle), dovitinib (DO 30 mg/kg or 60 mg/kg), or vandetanib (VA 50 mg/kg) for 32 days. Average percentage of change in tumor volume relative to initial tumor volume is shown. Error bars, SEM. ***, $P < 0.0001$ for vehicle (vehicle) versus dovitinib 30 mg/kg (DO 30 mg/kg) treatment group. B, waterfall plots showing the percent change in volume (relative to initial tumor volume) for the individual tumors in each treatment group. Maximum regression tumors for each group are indicated. C, mice bearing LC-2/ad cells expressing CCDC6–RET were orally administered a dose of 0 (Vehicle), 30 mg/kg, or 60 mg/kg dovitinib (DO), and 50 mg/kg vandetanib (VA). Tumors were collected and lysed at 6 hours postdosing. The expression levels of phospho-RET, RET, phospho-ERK, ERK, and β-actin were detected by Western blot analysis using the appropriate antibodies. D, immunohistochemical (IHC) analysis of LC-2/ad xenograft tumor samples. Mice were orally administered a dose of 0(vehicle), or 60 (dovitinib 60 mg/kg) for 6 hours and sacrificed, and tumors were stained with indicated antibodies. Photos shown are representative fields in each group in low and high magnification. Scale bars in the main images and in the insets indicate 100 and 50 μm, respectively.

Finally, concurrent inhibition of RET and Src signaling did not show synergistic antitumor effect in LC-2/ad DR cells, further supporting complete loss of dependence on RET signaling for survival upon acquisition of acquired resistance to dovitinib (Fig. 6E).

Given the activation of FAK and mRNA upregulation of integrin, we hypothesized that FAK–integrin axis was involved in the Src activation. To rule out this hypothesis, we used PF-562,271, ATP-competitive reversible inhibitor of FAK. Unexpectedly, PF-562,271 had neither antiproliferation effect nor inhibition of downstream ERK1/2 activation in LC-2/ad DR cells (Supplementary Fig. S3A and S3B). Expressions of integrins in LC-2/ad DR cells were similar with LC-2/ad cells (Supplementary Fig. S3C).

Taken together, these data indicate an essential role of Src in mediating the acquired resistance to dovitinib in *RET* fusion–positive LADC.

Discussion

In our study, we evaluated and compared antitumor activity of dovitinib in *RET* fusion–driven LADC models. Dovitinib efficiently suppressed growth of *RET*-rearranged LADC *in vitro* and *in vivo* by inhibiting autophosphorylation of RET and was shown to be at least as efficacious as other known RET–TKIs, such as sorafenib, sunitinib, and vandetanib. Our data provided the preclinical evidence supporting a rationale for the clinical development of dovitinib in patients with *RET*

Published OnlineFirst July 24, 2015; DOI: 10.1158/1535-7163.MCT-15-0350

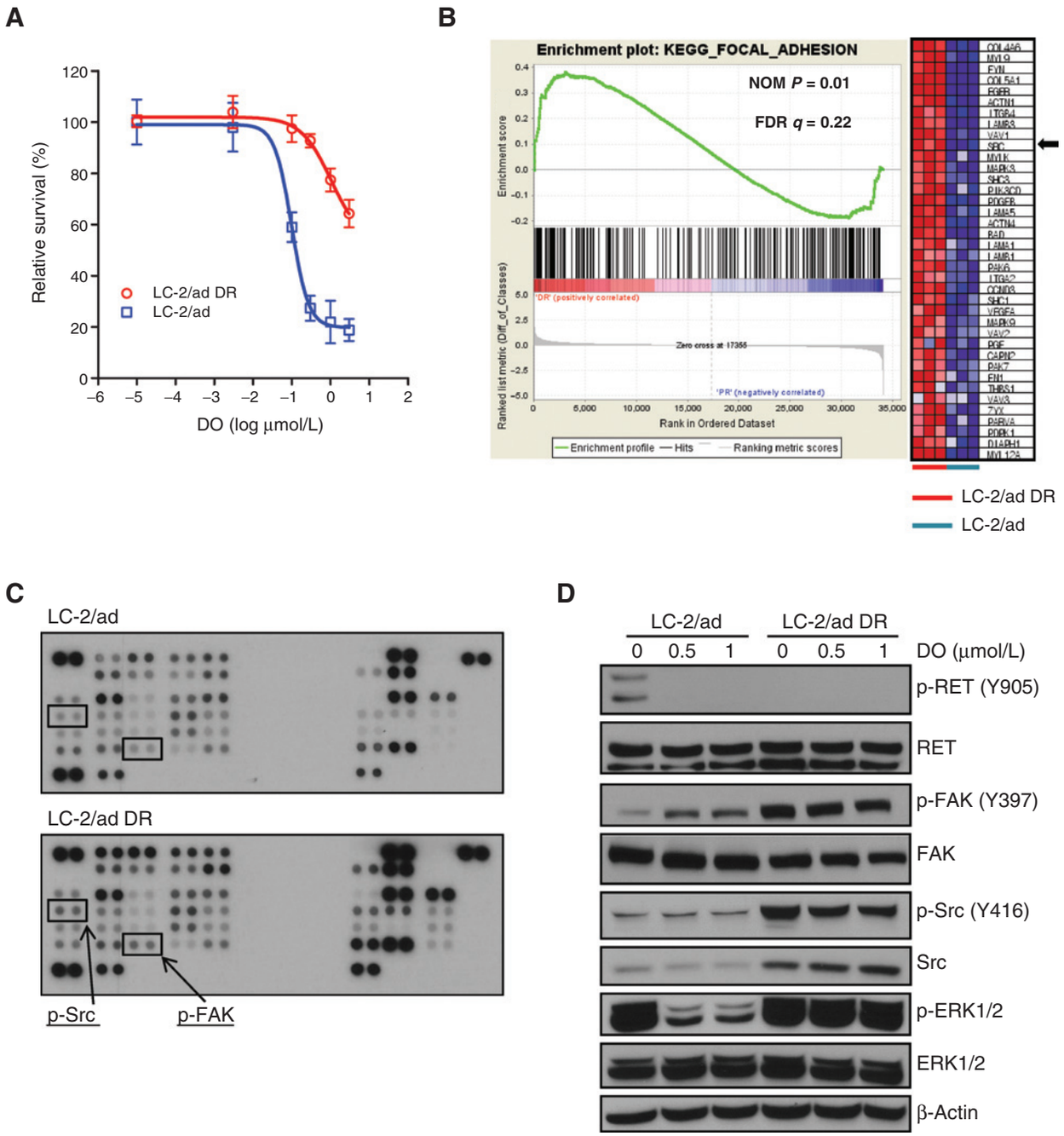

Figure 5.
Src hyperactivation in acquired dovitinib-resistant cells. A, MTT assay comparing cell proliferation of indicated parental LC-2/ad cells and their corresponding acquired dovitinib-resistant LC-2/ad DR cells upon treatment with dovitnib for 72 hours. B, the GSEA demonstrating a significant enrichment of the set of focal adhesion pathway genes among significantly differentially expressed genes between LC-2/ad and LC-2/ad DR cells. C, the phosphorylation state was detected by the R&D Systems Proteome Profiler Phospho-Kinase Array in LC-2/ad or LC-2/ad DR. Key activated kinases are indicated (FAK and Src). D, lysates from LC-2/ad and LC-2/ad DR cells were evaluated by Western blotting to determine total and phosphorylated protein levels from the arrays in C.

fusion–driven LADC. Furthermore, we found that increased activation of Src mediated acquired resistance to dovitinib by phosphorylating RET downstream effector ERK1/2 in *RET* fusion–positive LADC.

Given that *RET* rearrangement is a druggable target in LADC, a number of clinical trials have been designed to investigate the therapeutic effects of multikinase inhibitors targeting RET, such as vandetanib (trial registration ID: NCT01823068), sunitinib

Published OnlineFirst July 24, 2015; DOI: 10.1158/1535-7163.MCT-15-0350

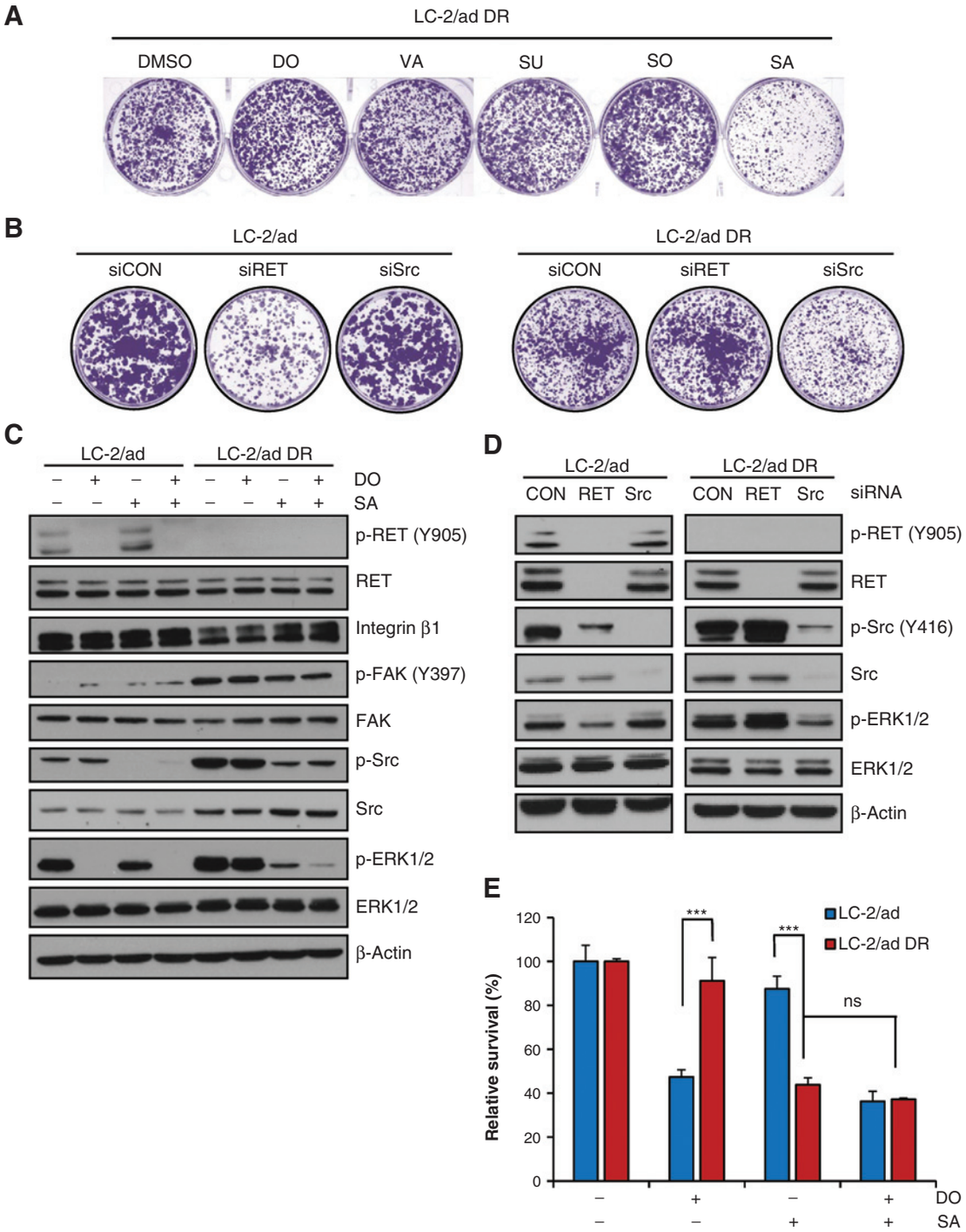

Figure 6.
Loss of dependency on RET-fusion and gain of dependency on Src in dovitinib-resistant cells. A, colony formation assay of LC-2/ad DR cells. Cells were grown in the absence or presence of 0.5 μmol/L dovitinib (DO), 0.5 μmol/L vandetanib (VA), 0.5 μmol/L sunitinib (SU), 0.5 μmol/L sorafenib (SO), or 0.5 μmol/L saracatinib (SA) for 14 days. All cells were fixed and stained with crystal violet (0.005%). B, colony formation assay of LC-2/ad and LC-2/ad DR cells. Cells were transfected with indicated siRNA and grown for 14 days. All cells were fixed and stained with crystal violet (0.005%). C, Western blot analysis assessing the effect of 1 μmol/L dovitinib (DO), 1 μmol/L saracatinib (SA), or combination treatment on LC-2/ad and LC-2/ad DR cells. Cells were treated indicated inhibitor(s) for 4 hours. Lysates were evaluated by Western blotting with the indicated antibodies. D, Western blot analysis of assessing the dependency, whether cell survival is mediated by *CCDC6–RET* or Src. Cells were transfected with siCON, siRET, or siSrc for 72 hours. Lysates were evaluated by Western blotting with the indicated antibodies. E, MTT assay of single or combination treatment of 1 μmol/L dovitinib (DO) and 1 μmol/L saracatinib (SA) in LC-2/ad and LC-2/ad DR cells. LC-2/ad and LC-2/ad DR cells were incubated for 72 hours with indicated inhibitors before treating with MTT solution. Error bars, mean ± SE of three replicates. ***, $P < 0.001$, dovitinib (DO)- or saracatinib (SA)-treated LC-2/ad versus LC-2/ad DR; ns, not significant, saracatinib (SA)-treated LC-2/ad DR versus combination-treated LC-2/ad DR.

Published OnlineFirst July 24, 2015; DOI: 10.1158/1535-7163.MCT-15-0350

(NCT01829217), cabozantinib (NCT01639508), and lenvatinib (NCT01877083), in *RET* fusion–positive LADC. In a recent report of preliminary efficacy in patients with *RET* fusion–positive LADC, cabozantinib, an inhibitor of MET, VEGFR and RET, achieved partial responses in 2 patients and durable stable disease in 1 patient (12). Vandetanib, an inhibitor of VEGFR, EGFR, and RET, showed a dramatic response in a patients with advanced *RET* fusion–positive LADC (16). Moreover, alectinib (CH5424802), which has been known to be a selective inhibitor of ALK, showed antitumor activity against *RET* fusion–driven LADC models by inhibiting oncogenic RET fusion signaling (23). Our data support the inclusion of dovitinib in the therapeutic armamentarium of targeted agents currently being tested for *RET* fusion–positive LADC. On the basis of our *in vitro* data, the lowest effective dose of dovitinib in LC-2/ad cells was 0.1 μmol/L (Fig. 2A and B, Supplementary Fig. S1A), which can be extrapolated to 48.25 ng/mL. In our study, dovitinib showed significant anti-tumor effect in the LC-2/ad xenograft at the dose of 30 mg/kg dovitinib. The trough plasma concentration (C_{min}) of 7 to 23 ng/mL (20–60 nmol/L) were observed *in vivo* with 30 mg/kg dovitinib doses, and the corresponding C_{max} and AUC values ranged from 339 to 952 ng/mL and 5,540 to 9,670 h•ng/mL, respectively (18). Dovitinib showed pharmacodynamics effect in this dose concentration range. This information suggests that the corresponding plasma exposures were adequate for substantial efficacy in the LC-2/ad xenograft model. Moreover, dovitinib has been evaluated in human phase I studies and was shown to have C_{max} 273 ± 126 ng/mL at steady state of recommended dose (500 mg, 5 days on, 2 days off; refs. 18, 24). These results suggest that preclinical doses tested in our study can safely be achieved in patients with *RET*-rearranged lung adenocarcinoma.

Targeted agents that exploit genetic vulnerabilities in human cancers have now been clinically validated as effective cancer therapies. However, clinical efficacy of these agents is limited by the rapid emergence of drug resistance, which remains a substantial challenge to the clinical management of advanced cancers (21, 25–28). To our knowledge, this is the first report on the mechanism of acquired resistance to the *RET* inhibitor describing a link between Src-dependent survival signal activation and drug resistance in *RET* fusion–positive LADC.

Src regulates many fundamental cellular processes, including cell growth, differentiation, migration, and drug resistance (22, 29–32). In our study, acquisition of acquired resistance to dovitinib is attributable to the activation of a Src-driven bypass signaling pathway. We observed marked activation and expression of Src in LC-2/ad DR cells, as compared with the LC-2/ad cells. The blockade of Src signaling by saracatinib or siSrc resulted in the marked suppression of ERK1/2 phosphorylation, suggesting a dominant role of Src on ERK1/2 activation in LC-2/ad DR cells. Consistent with these results, treatment with saracatinib and siSrc dramatically suppressed cell growth in LC-2/ad DR cells. The disappointing lack of synergy in the combined treatment of dovitinib and saracatinib may be due to the fact that survival of LC-2/ad DR cells no longer depend on the activity of RET fusion kinase (Figs. 5D and 6E). Similar to our findings, loss of addiction to mutant EGFR resulted in gain of addiction to both HER2/HER3 and PI3K/Akt signaling to acquire EGFR–TKI resistance (33).

Integrins are a family of adhesion receptors for extracellular matrix (ECM) proteins, integrins can transduce biochemical signals into the cell to regulate a variety of cellular functions, including proliferation, migration, survival, and drug resistance (34–37). Focal adhesion kinase (FAK) is a nonreceptor tyrosine kinase that mediates integrin signaling pathways. Src family of cytosolic protein tyrosine kinases function intimately with FAK in integrin signaling pathways (38, 39). In our study, FAK activity was increased in LC-2/ad DR cells (Fig. 5D). These data also raise the question as to whether FAK could play an important role in the enhanced Src activation, resulting in the acquisition of dovitinib resistance in LC-2/ad DR cells. However, the inhibition of FAK activity using PF-562,271 could not suppress the downstream ERK1/2 activation and LC-2/ad DR cell growth (Supplementary Fig. S3A and S3B). As shown in Supplementary Fig. S3C, protein levels of integrins in LC-2/ad DR cells were similar with LC-2/ad cells and treatment of intergrinβ1 could not inhibit the cell growth in LC-2/ad DR cells (data not shown). These data suggest that integrin-mediated FAK activation may not be critically involved in acquired resistance to dovitinib in LC-2/ad DR cell. Instead, Src, as a common node downstream of multiple drug resistance pathways, might be activated by various signal inputs from specific RTKs, nonreceptor tyrosine kinases, or loss of protein tyrosine phosphatase activity (29, 31). Therefore, it remains to be further studied what mediates the enhanced activity of Src.

In conclusion, our findings support that dovitinib warrants further clinical evaluation in patients with *RET*-rearranged LADC, and targeting Src signaling is effective in *RET*-rearranged LADC with acquired resistance to dovitinib.

Disclosure of Potential Conflicts of Interest

No potential conflicts of interest were disclosed.

Authors' Contributions

Conception and design: C.W. Kang, K.W. Jang, H.R. Kim, S.M. Lim, S.M. Lim, S. Paik, D.J. Kim, J.H. Kim, B.C. Cho

Development of methodology: C.W. Kang, K.W. Jang, J. Sohn, B.C. Cho

Acquisition of data (provided animals, acquired and managed patients, provided facilities, etc.): C.W. Kang, K.W. Jang, J. Sohn, S.M. Lim, S.M. Lim, Y.W. Moon, S. Paik, J.H. Kim, B.C. Cho

Analysis and interpretation of data (e.g., statistical analysis, biostatistics, computational analysis): C.W. Kang, K.W. Jang, S.-M. Kim, K.-H. Pyo, M.R. Yun, S.M. Lim, S. Paik, B.C. Cho

Writing, review, and/or revision of the manuscript: C.W. Kang, S.M. Lim, S. Paik, J.H. Kim, B.C. Cho

Administrative, technical, or material support (i.e., reporting or organizing data, constructing databases): C.W. Kang, K.W. Jang, J. Sohn, J.H. Kim, K.-H. Pyo, B.C. Cho

Study supervision: C.W. Kang, K.W. Jang, H. Kim, H.N. Kang, S. Paik, D.J. Kim, B.C. Cho

Grant Support

This work was supported by the National Research Foundation of Korea (NRF) funded by the Korean government (MEST; 2012R1A2A2A01046927; to B.C. Cho) and a grant of the Korea Health Technology R&D Project through the Korea Health Industry Development Institute (KHIDI), funded by the Ministry of Health and Welfare, Republic of Korea (HI13C2162; to S. Paik).

The costs of publication of this article were defrayed in part by the payment of page charges. This article must therefore be hereby marked *advertisement* in accordance with 18 U.S.C. Section 1734 solely to indicate this fact.

Received May 1, 2015; revised July 1, 2015; accepted July 5, 2015; published OnlineFirst July 24, 2015.

Published OnlineFirst July 24, 2015; DOI: 10.1158/1535-7163.MCT-15-0350

References

1. Lee YJ, Kim JH, Kim SK, Ha SJ, Mok TS, Mitsudomi T, et al. Lung cancer in never smokers: change of a mindset in the molecular era. Lung Cancer 2011;72:9–15.
2. Pao W, Girard N. New driver mutations in non-small-cell lung cancer. Lancet Oncol 2011;12:175–80.
3. Mok TS, Wu YL, Thongprasert S, Yang CH, Chu DT, Saijo N, et al. Gefitinib or carboplatin-paclitaxel in pulmonary adenocarcinoma. N Engl J Med 2009;361:947–57.
4. Kwak EL, Bang YJ, Camidge DR, Shaw AT, Solomon B, Maki RG, et al. Anaplastic lymphoma kinase inhibition in non-small-cell lung cancer. N Engl J Med 2010;363:1693–703.
5. Maemondo M, Inoue A, Kobayashi K, Sugawara S, Oizumi S, Isobe H, et al. Gefitinib or chemotherapy for non-small-cell lung cancer with mutated EGFR. N Engl J Med 2010;362:2380–8.
6. Wang R, Hu H, Pan Y, Li Y, Ye T, Li C, et al. RET fusions define a unique molecular and clinicopathologic subtype of non-small-cell lung cancer. J Clin Oncol 2012;30:4352–9.
7. Kohno T, Ichikawa H, Totoki Y, Yasuda K, Hiramoto M, Nammo T, et al. KIF5B-RET fusions in lung adenocarcinoma. Nat Med 2012;18:375–7.
8. Takeuchi K, Soda M, Togashi Y, Suzuki R, Sakata S, Hatano S, et al. RET, ROS1 and ALK fusions in lung cancer. Nat Med 2012;18:378–81.
9. Cai W, Su C, Li X, Fan L, Zheng L, Fei K, et al. KIF5B-RET fusions in Chinese patients with non-small cell lung cancer. Cancer 2013;119:1486–94.
10. Lipson D, Capelletti M, Yelensky R, Otto G, Parker A, Jarosz M, et al. Identification of new ALK and RET gene fusions from colorectal and lung cancer biopsies. Nat Med 2012;18:382–4.
11. Garcia MV, Cho BC. Copy number abnormalities and gene fusions in lung cancer: present and developing technologies. In:Harvey I. Pass DB, Scagliotti Giorgio V., editors. The IASLC multidisciplinary approach to thoracic oncology. Aurora, CO: International Association for the Study of Lung Cancer; 2014. p. 137–9.
12. Drilon A, Wang L, Hasanovic A, Suehara Y, Lipson D, Stephens P, et al. Response to Cabozantinib in patients with RET fusion-positive lung adenocarcinomas. Cancer Discov 2013;3:630–5.
13. Yokota K, Sasaki H, Okuda K, Shimizu S, Shitara M, Hikosaka Y, et al. KIF5B/RET fusion gene in surgically-treated adenocarcinoma of the lung. Oncol Rep 2012;28:1187–92.
14. Suzuki M, Makinoshima H, Matsumoto S, Suzuki A, Mimaki S, Matsushima K, et al. Identification of a lung adenocarcinoma cell line with CCDC6-RET fusion gene and the effect of RET inhibitors *in vitro* and *in vivo*. Cancer Sci 2013;104:896–903.
15. Matsubara D, Kanai Y, Ishikawa S, Ohara S, Yoshimoto T, Sakatani T, et al. Identification of CCDC6-RET fusion in the human lung adenocarcinoma cell line, LC-2/ad. J Thorac Oncol 2012;7:1872–6.
16. Falchook GS, Ordonez NG, Bastida CC, Stephens PJ, Miller VA, Gaido L, et al. Effect of the RET inhibitor vandetanib in a patient with RET fusion-positive metastatic non-small-cell lung cancer. J Clin Oncol 2014;32:1–3.
17. Kutluk Cenik B, Ostapoff KT, Gerber DE, Brekken RA. BIBF 1120 (nintedanib), a triple angiokinase inhibitor, induces hypoxia but not EMT and blocks progression of preclinical models of lung and pancreatic cancer. Mol Cancer Ther 2013;12:992–1001.
18. Angevin E, Lopez-Martin JA, Lin CC, Gschwend JE, Harzstark A, Castellano D, et al. Phase I study of dovitinib (TKI258), an oral FGFR, VEGFR, and PDGFR inhibitor, in advanced or metastatic renal cell carcinoma. Clin Cancer Res 2013;19:1257–68.
19. Azab AK, Azab F, Quang P, Maiso P, Sacco A, Ngo HT, et al. FGFR3 is overexpressed waldenstrom macroglobulinemia and its inhibition by Dovitinib induces apoptosis and overcomes stroma-induced proliferation. Clin Cancer Res 2011;17:4389–99.
20. Edgar R, Domrachev M, Lash AE. Gene Expression Omnibus: NCBI gene expression and hybridization array data repository. Nucleic Acids Res 2002;30:207–10.
21. Pao W, Miller VA, Politi KA, Riely GJ, Somwar R, Zakowski MF, et al. Acquired resistance of lung adenocarcinomas to gefitinib or erlotinib is associated with a second mutation in the EGFR kinase domain. PLoS Med 2005;2:e73.
22. Crystal AS, Shaw AT, Sequist LV, Friboulet L, Niederst MJ, Lockerman EL, et al. Patient-derived models of acquired resistance can identify effective drug combinations for cancer. Science 2014;346:1480–6.
23. Kodama T, Tsukaguchi T, Satoh Y, Yoshida M, Watanabe Y, Kondoh O, et al. Alectinib shows potent antitumor activity against RET-rearranged non-small cell lung cancer. Mol Cancer Ther 2014;13:2910–8.
24. Sarker D, Molife R, Evans TR, Hardie M, Marriott C, Butzberger-Zimmerli P, et al. A phase I pharmacokinetic and pharmacodynamic study of TKI258, an oral, multitargeted receptor tyrosine kinase inhibitor in patients with advanced solid tumors. Clin Cancer Res 2008;14:2075–81.
25. Lackner MR, Wilson TR, Settleman J. Mechanisms of acquired resistance to targeted cancer therapies. Fut Oncol 2012;8:999–1014.
26. Engelman JA, Zejnullahu K, Mitsudomi T, Song Y, Hyland C, Park JO, et al. MET amplification leads to gefitinib resistance in lung cancer by activating ERBB3 signaling. Science 2007;316:1039–43.
27. Shi H, Moriceau G, Kong X, Lee MK, Lee H, Koya RC, et al. Melanoma whole-exome sequencing identifies (V600E)B-RAF amplification-mediated acquired B-RAF inhibitor resistance. Nat Commun 2012;3:724.
28. Wagle N, Emery C, Berger MF, Davis MJ, Sawyer A, Pochanard P, et al. Dissecting therapeutic resistance to RAF inhibition in melanoma by tumor genomic profiling. J Clin Oncol 2011;29:3085–96.
29. Zhang S, Huang WC, Li P, Guo H, Poh SB, Brady SW, et al. Combating trastuzumab resistance by targeting SRC, a common node downstream of multiple resistance pathways. Nat Med 2011;17:461–9.
30. Kanda R, Kawahara A, Watari K, Murakami Y, Sonoda K, Maeda M, et al. Erlotinib resistance in lung cancer cells mediated by integrin beta1/Src/Akt-driven bypass signaling. Cancer Res 2013;73:6243–53.
31. Yeatman TJ. A renaissance for SRC. Nat Rev Cancer 2004;4:470–80.
32. Girotti MR, Pedersen M, Sanchez-Laorden B, Viros A, Turajlic S, Niculescu-Duvaz D, et al. Inhibiting EGF receptor or SRC family kinase signaling overcomes BRAF inhibitor resistance in melanoma. Cancer Discov 2013;3:158–67.
33. Tabara K, Kanda R, Sonoda K, Kubo T, Murakami Y, Kawahara A, et al. Loss of activating EGFR mutant gene contributes to acquired resistance to EGFR tyrosine kinase inhibitors in lung cancer cells. PLoS ONE 2012;7:e41017.
34. Seguin L, Desgrosellier JS, Weis SM, Cheresh DA. Integrins and cancer: regulators of cancer stemness, metastasis, and drug resistance. Trends Cell Biol 2015;25:234–240.
35. Huang C, Park CC, Hilsenbeck SG, Ward R, Rimawi MF, Wang YC, et al. beta1 integrin mediates an alternative survival pathway in breast cancer cells resistant to lapatinib. Breast Cancer Res 2011;13:R84.
36. Schober M, Fuchs E. Tumor-initiating stem cells of squamous cell carcinomas and their control by TGF-beta and integrin/focal adhesion kinase (FAK) signaling. Proc Natl Acad Sci U S A 2011;108:10544–9.
37. Damiano JS, Cress AE, Hazlehurst LA, Shtil AA, Dalton WS. Cell adhesion mediated drug resistance (CAM-DR): role of integrins and resistance to apoptosis in human myeloma cell lines. Blood 1999;93:1658–67.
38. Sulzmaier FJ, Jean C, Schlaepfer DD. FAK in cancer: mechanistic findings and clinical applications. Nat Rev Cancer 2014;14:598–610.
39. Frame MC, Serrels A. FAK to the rescue: activated stroma promotes a "Safe Haven" for BRAF-mutant melanoma cells by inducing FAK signaling. Cancer Cell 2015;27:429–31.

Published OnlineFirst July 24, 2015; DOI: 10.1158/1535-7163.MCT-15-0350

AACR American Association for Cancer Research

Molecular Cancer Therapeutics

Antitumor Activity and Acquired Resistance Mechanism of Dovitinib (TKI258) in *RET*-Rearranged Lung Adenocarcinoma

Chan Woo Kang, Kang Won Jang, Jinyoung Sohn, et al.

Mol Cancer Ther 2015;14:2238-2248. Published OnlineFirst July 24, 2015.